

Supplementary Materials

Mechanism of the influence of thermal aging on flame-retardant microcapsulated phase-change materials for battery thermal safety

Gengfeng Zhao¹, Jian Deng¹, Beiwen Liang¹, Tingyu Wang², Wen Luo¹, Jiexin Du², Hongli Liu³, Wensheng Yang¹, Yingbang Yao¹, Zikai Guo¹, Zhipeng Sun¹, Xixi Li^{1,*}

¹School of Materials and Energy, Guangdong University of Technology, Guangzhou 510006, Guangdong, China.

²School of Ocean Engineering, Guangzhou Maritime University, Guangzhou 510725, Guangdong, China.

³College of Aeronautical Engineering, Civil Aviation University of China, Tianjin, 300300, China

***Correspondence to:** Prpf. Xixi Li, School of Materials and Energy, Guangdong University of Technology, Guangzhou 510006, Guangdong, China. E-mail: pkdlxx@gdut.edu.cn

The supporting figures and tables are listed as follow:

Fig. S1

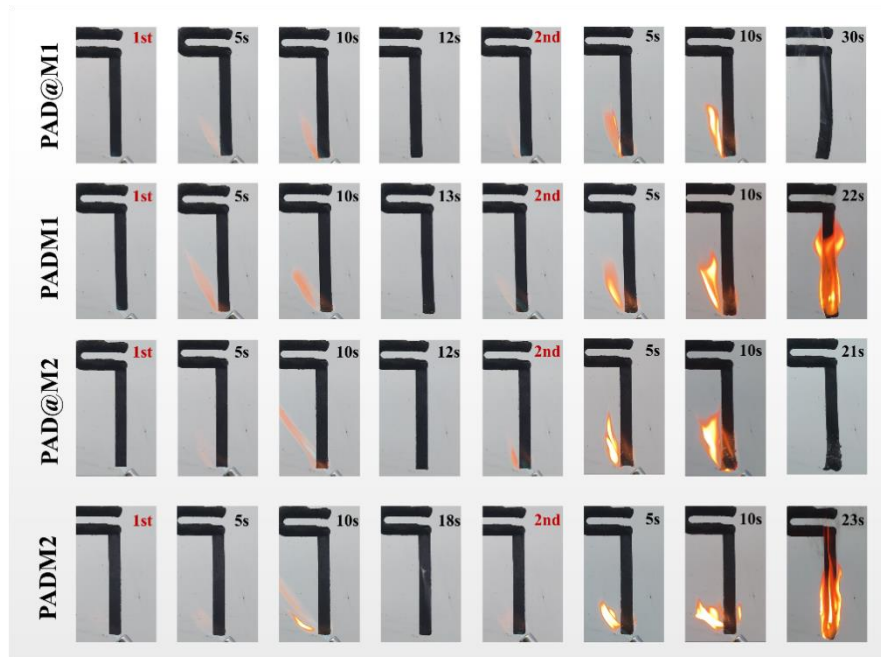


Fig. S1 Vertical Flame Test of different CPCM.

PAD@M1 self-extinguished at 12 seconds after the first ignition and at 30 seconds after the second ignition, achieving a V-1 rating. PADM1 self-extinguished at 13 seconds after the first ignition but continued to burn until 22 seconds during the second ignition, failing to meet the UL-94 standard. PAD@M2 self-extinguished at 12 seconds and 20 seconds after the first and second ignitions, respectively, also rated as V-1. PADM2 self-extinguished at 18 seconds after the first ignition but failed to self-extinguish by 23 seconds after the second ignition.

SI 2.1 Thermal properties

The thermal behavior of CPCMs was analyzed using DSC (Q2000, TA Instruments, USA). Tests were conducted under a nitrogen purge at 50 mL/min, with heating and cooling rates set to 10 °C/min across a temperature span of 20–80 °C. The latent heat (ΔH) was calculated by integrating peak areas via Universal Analysis 2000, following prior indium calibration.

Energy Materials

Thermal conductivity was measured using the transient plane source (TPS) method via a Hot Disk TPS 500s analyzer (Hot Disk AB, Sweden; accuracy $\pm 3\%$). CPCM samples (15 mm in diameter and 5 mm thick) were finely polished ($R_a < 0.1 \mu\text{m}$) to ensure flat surfaces and placed symmetrically on both sides of the Kapton-insulated sensor. A three-point contact method was employed to reduce thermal contact resistance, and each measurement was repeated five times at 25 °C to enhance reliability.

SI 2.2 Flame retardant properties

The fire resistance of CPCMs was assessed through multi-standard combustion tests, including vertical burning in compliance with UL-94 using a cone calorimeter (FTT, Fire Testing Technology, UK). Type V specimens ($125 \times 13 \times 3.2 \text{ mm}^3$) were vertically clamped and exposed to a methane flame (50 W ignition source). Each material's flammability rating (V-0 to V-2 classification) was determined as the average of five independent trials, with post-combustion dripping behavior recorded via high-speed imaging.

Limiting oxygen index (LOI, NETZSCH, Germany) measurements were performed following EN 45545-2:2013/A1:2015 guidelines using a Stanton Redcroft FTA oxygen index analyzer. Test bars ($125 \times 6.5 \times 3.2 \text{ mm}^3$) were vertically mounted in a controlled oxygen/nitrogen atmosphere, with LOI values calculated as the minimum oxygen concentration supporting candle-like combustion. Ten replicates per formulation were tested to ensure statistical reliability.

Combustion kinetics were further assessed using ISO 5660-compliant cone calorimetry (FTT Cone Calorimeter, Fire Testing Technology, UK) under an external heat flux of 35 kW/m². Square specimens ($100 \times 100 \times 3.2 \text{ mm}^3$) were horizontally irradiated with simultaneous monitoring of total smoke production (TSP), heat release rate (HRR), and carbon monoxide yield. Triplicate measurements were conducted at 25 °C and 50% relative humidity.

Energy Materials

Post-combustion residue analysis was performed using field-emission SEM (SU8010, Hitachi High-Tech, Japan). Char layers were sputter-coated with 5 nm platinum before imaging to enhance surface conductivity.

SI 2.3 Thermal management and thermal propagation measurements of battery module

A commercial lithium nickel manganese cobalt oxide (NMC) battery with a nominal capacity of 20 Ah was used as the test platform. Table 2 presents the specifications of both the battery and its module. Individual cells were welded and configured into modules using a 2P×3S arrangement.

To investigate the thermal regulation performance of flame retardant CPCM before and after thermal cycling, four types of battery modules PAD@M3, PADM3, Aged PAD@M3, and Aged PADM3 were designed. They are denoted as PAD@M3-module, PADM3-module, Aged-PAD@M3-module, Aged-PADM3-module, respectively. The BTM system is shown in Fig. 2a. Further, the Table 3 presents the charge and discharge test conditions and the corresponding thermal management evaluation results. Besides, the propagation behavior within the module was visually tracked using an infrared camera (TiS60, Fluke Corporation, USA). Additional test apparatus is illustrated in Fig. 2(b).

It included a battery cycler (BTS-NTF, Neware Electronics Co., Ltd., Shenzhen, China), a temperature–humidity chamber (Bell Test Equipment Co., Ltd., Dongguan, China), a data acquisition unit (Agilent Technologies, USA), the module, and a computer. The battery module was placed in an incubator at 25°C, and cyclic charge–discharge tests were performed at different rates using a battery test system.

Meanwhile, the Agilent instrument was also employed to track changes in the battery surface temperature. In this work, the maximum temperature difference in the module, ΔT_{max} , is defined as the maximum instantaneous temperature difference between the center battery and the side batteries during the charge–discharge process, which can

be expressed as:

$$\Delta T_{max} = \max(T_{center} - T_{side}) \quad (1)$$

where T_{center} represents the temperature measured at the side center of the center battery, and T_{side} represents the temperature measured at the side center of the leftmost battery in the module. Table 3 presents the charge–discharge test conditions and the corresponding thermal management evaluation results.

Besides, TR in battery modules, often precipitated by progressive heat accumulation, poses critical safety risks through potential combustion and explosion events, particularly in electric vehicles and marine battery systems. flame retardant CPCMs demonstrate vital multimodal functionality by simultaneously mitigating thermal runaway initiation through phase-change enthalpy absorption and suppressing post-runaway combustion via intumescent char formation, thus significantly improving the thermal safety of battery-powered transport vehicles. In the experiment, a stainless steel heating plate (100 mm×20 mm×140 mm, l×w×h) was employed to mimic the exothermic onset of a single battery TR event. A 200 W DC power supply was used for heating, and an Agilent system recorded temperature variations. the propagation behavior within the module was visually tracked using an infrared camera (TiS60, Fluke Corporation, USA). Additional test apparatus is illustrated in Fig. 2(b).